Lattice QCD constraints on the QCD critical point

Alexei Bazavov

Michigan State University

June 2, 2018

Introduction

- QCD phase diagram
- Lattice gauge theory
- Challenges

Results at $\mu_B = 0$

- Chiral symmetry restoration

Results at $\mu_B > 0$

- Curvature of the crossover line
- The equation of state at $O(\mu_B^6)$
- Freeze-out parameters
- Constraints on the critical point

Conclusion

(Conjectured) QCD phase diagram

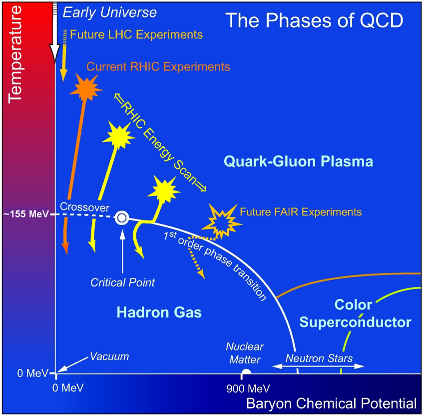

[1] Collins, Perry (1975), Cabbibo, Parisi (1975)

(Conjectured) QCD phase diagram

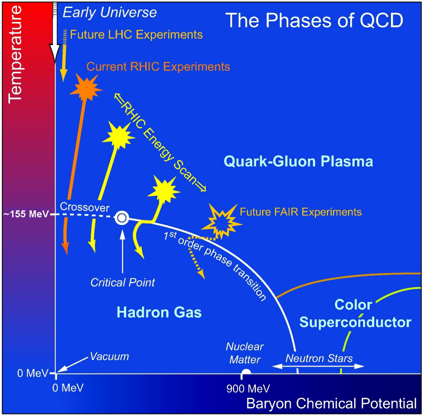

- Study response of the system to change of external parameters, i.e. temperature and baryon density, asymptotic freedom suggests a weakly interacting phase[1]

[1] Collins, Perry (1975), Cabbibo, Parisi (1975)

(Conjectured) QCD phase diagram

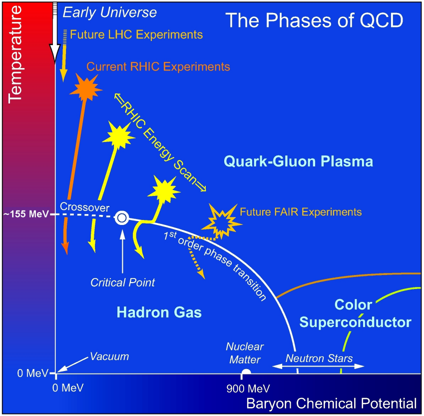

- Study response of the system to change of external parameters, i.e. temperature and baryon density, asymptotic freedom suggests a weakly interacting phase[1]
- Experimental program: RHIC, LHC, FAIR, NICA

[1] Collins, Perry (1975), Cabbibo, Parisi (1975)

(Conjectured) QCD phase diagram

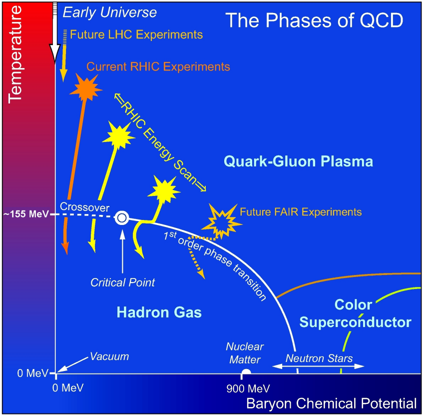

- Study response of the system to change of external parameters, i.e. temperature and baryon density, asymptotic freedom suggests a weakly interacting phase[1]
- Experimental program: RHIC, LHC, FAIR, NICA
- RHIC BES: search for the critical point

[1] Collins, Perry (1975), Cabbibo, Parisi (1975)

(Conjectured) QCD phase diagram

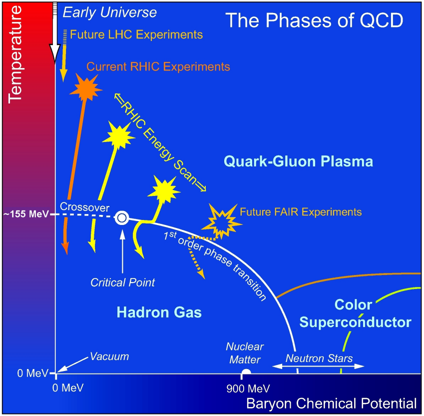

- Study response of the system to change of external parameters, i.e. temperature and baryon density, asymptotic freedom suggests a weakly interacting phase[1]
- Experimental program: RHIC, LHC, FAIR, NICA
- RHIC BES: search for the critical point

- First-principle calculations are possible at $\mu_B/T = 0$, expansions/extrapolations at small μ_B/T

[1] Collins, Perry (1975), Cabbibo, Parisi (1975)

Lattice gauge theory

- Start with the path integral quantization, Euclidean signature:

$$
\begin{aligned}
\langle \mathcal{O} \rangle &= \frac{1}{\mathcal{Z}} \int \mathcal{D}[\psi]\mathcal{D}[\bar{\psi}]\mathcal{D}[A]\ \mathcal{O} \exp(-\mathcal{S}_E(T, V, \vec{\mu})), \\
\mathcal{Z}(T, V, \vec{\mu}) &= \int \mathcal{D}[\psi]\mathcal{D}[\bar{\psi}]\mathcal{D}[A] \exp(-\mathcal{S}_E(T, V, \vec{\mu})),
\end{aligned}
$$

Lattice gauge theory

- Start with the path integral quantization, Euclidean signature:

$$
\begin{aligned}
\langle \mathcal{O} \rangle &= \frac{1}{\mathcal{Z}} \int \mathcal{D}[\psi]\mathcal{D}[\bar{\psi}]\mathcal{D}[A]\ \mathcal{O} \exp(-\mathcal{S}_E(T,V,\vec{\mu})), \\
\mathcal{Z}(T,V,\vec{\mu}) &= \int \mathcal{D}[\psi]\mathcal{D}[\bar{\psi}]\mathcal{D}[A] \exp(-\mathcal{S}_E(T,V,\vec{\mu})), \\
\mathcal{S}_E(T,V,\vec{\mu}) &= -\int_0^{1/T} dx_0 \int_V d^3\mathbf{x}\mathcal{L}^E(\vec{\mu}),
\end{aligned}
$$

Lattice gauge theory

- Start with the path integral quantization, Euclidean signature:

$$
\begin{aligned}
\langle \mathcal{O} \rangle &= \frac{1}{\mathcal{Z}} \int \mathcal{D}[\psi]\mathcal{D}[\bar{\psi}]\mathcal{D}[A]\ \mathcal{O} \exp(-\mathcal{S}_E(T, V, \vec{\mu})), \\
\mathcal{Z}(T, V, \vec{\mu}) &= \int \mathcal{D}[\psi]\mathcal{D}[\bar{\psi}]\mathcal{D}[A] \exp(-\mathcal{S}_E(T, V, \vec{\mu})), \\
\mathcal{S}_E(T, V, \vec{\mu}) &= -\int_0^{1/T} dx_0 \int_V d^3\mathbf{x} \mathcal{L}^E(\vec{\mu}), \\
\mathcal{L}^E(\vec{\mu}) &= \mathcal{L}^E_{QCD} + \sum_{f=u,d,s} \mu_f \bar{\psi}_f \gamma_0 \psi_f
\end{aligned}
$$

Lattice gauge theory

- Start with the path integral quantization, Euclidean signature:

$$\begin{aligned}
\langle \mathcal{O} \rangle &= \frac{1}{\mathcal{Z}} \int \mathcal{D}[\psi]\mathcal{D}[\bar{\psi}]\mathcal{D}[A]\ \mathcal{O} \exp(-\mathcal{S}_E(T, V, \vec{\mu})), \\
\mathcal{Z}(T, V, \vec{\mu}) &= \int \mathcal{D}[\psi]\mathcal{D}[\bar{\psi}]\mathcal{D}[A] \exp(-\mathcal{S}_E(T, V, \vec{\mu})), \\
\mathcal{S}_E(T, V, \vec{\mu}) &= -\int_0^{1/T} dx_0 \int_V d^3\mathbf{x} \mathcal{L}^E(\vec{\mu}), \\
\mathcal{L}^E(\vec{\mu}) &= \mathcal{L}^E_{QCD} + \sum_{f=u,d,s} \mu_f \bar{\psi}_f \gamma_0 \psi_f
\end{aligned}$$

- Introduce a (non-perturbative!) regulator – minimum space-time "resolution" scale a, i.e. lattice, Wilson (1974)

Lattice gauge theory

- Start with the path integral quantization, Euclidean signature:

$$
\begin{aligned}
\langle \mathcal{O} \rangle &= \frac{1}{\mathcal{Z}} \int \mathcal{D}[\psi]\mathcal{D}[\bar{\psi}]\mathcal{D}[A]\ \mathcal{O} \exp(-\mathcal{S}_E(T,V,\vec{\mu})), \\
\mathcal{Z}(T,V,\vec{\mu}) &= \int \mathcal{D}[\psi]\mathcal{D}[\bar{\psi}]\mathcal{D}[A] \exp(-\mathcal{S}_E(T,V,\vec{\mu})), \\
\mathcal{S}_E(T,V,\vec{\mu}) &= -\int_0^{1/T} dx_0 \int_V d^3\mathbf{x} \mathcal{L}^E(\vec{\mu}), \\
\mathcal{L}^E(\vec{\mu}) &= \mathcal{L}^E_{QCD} + \sum_{f=u,d,s} \mu_f \bar{\psi}_f \gamma_0 \psi_f
\end{aligned}
$$

- Introduce a (non-perturbative!) regulator – minimum space-time "resolution" scale a, i.e. lattice, Wilson (1974)
- The lattice spacing a acts as a UV cutoff, $p_{max} \sim \pi/a$

Lattice gauge theory

- Start with the path integral quantization, Euclidean signature:

$$
\begin{aligned}
\langle \mathcal{O} \rangle &= \frac{1}{\mathcal{Z}} \int \mathcal{D}[\psi]\mathcal{D}[\bar{\psi}]\mathcal{D}[A]\ \mathcal{O} \exp(-\mathcal{S}_E(T,V,\vec{\mu})), \\
\mathcal{Z}(T,V,\vec{\mu}) &= \int \mathcal{D}[\psi]\mathcal{D}[\bar{\psi}]\mathcal{D}[A] \exp(-\mathcal{S}_E(T,V,\vec{\mu})), \\
\mathcal{S}_E(T,V,\vec{\mu}) &= -\int_0^{1/T} dx_0 \int_V d^3\mathbf{x} \mathcal{L}^E(\vec{\mu}), \\
\mathcal{L}^E(\vec{\mu}) &= \mathcal{L}^E_{QCD} + \sum_{f=u,d,s} \mu_f \bar{\psi}_f \gamma_0 \psi_f
\end{aligned}
$$

- Introduce a (non-perturbative!) regulator – minimum space-time "resolution" scale a, i.e. lattice, Wilson (1974)
- The lattice spacing a acts as a UV cutoff, $p_{max} \sim \pi/a$
- The integrals can be evaluated with importance sampling methods

Challenges

- Broken symmetries – e.g., Lorentz, chiral

Challenges

- Broken symmetries – e.g., Lorentz, chiral
- Fermion doubling

Challenges

- Broken symmetries – e.g., Lorentz, chiral
- Fermion doubling
- Grassmann fields (fermions) cannot be sampled, integrate them out:

$$\begin{aligned}\mathcal{Z} &= \int \mathcal{D}[U]\mathcal{D}[\psi]\mathcal{D}[\bar{\psi}]e^{-\mathcal{S}_G[U]-\mathcal{S}_F[\bar{\psi},\psi,U]} \\ &= \int \mathcal{D}[U]e^{-\mathcal{S}_G[U]}\,\det|M[U]|\end{aligned}$$

Challenges

- Broken symmetries – e.g., Lorentz, chiral
- Fermion doubling
- Grassmann fields (fermions) cannot be sampled, integrate them out:

$$\mathcal{Z} = \int \mathcal{D}[U]\mathcal{D}[\psi]\mathcal{D}[\bar{\psi}]e^{-\mathcal{S}_G[U]-\mathcal{S}_F[\bar{\psi},\psi,U]}$$
$$= \int \mathcal{D}[U]e^{-\mathcal{S}_G[U]} \det |M[U]|$$

- The effective action is highly non-local, Monte Carlo sampling is costly
- The computational cost is determined by the condition number of the fermion matrix, which scales with the inverse lightest quark mass

Challenges

- Broken symmetries – e.g., Lorentz, chiral
- Fermion doubling
- Grassmann fields (fermions) cannot be sampled, integrate them out:

$$\mathcal{Z} = \int \mathcal{D}[U]\mathcal{D}[\psi]\mathcal{D}[\bar{\psi}]e^{-\mathcal{S}_G[U]-\mathcal{S}_F[\bar{\psi},\psi,U]}$$
$$= \int \mathcal{D}[U]e^{-\mathcal{S}_G[U]} \det|M[U]|$$

- The effective action is highly non-local, Monte Carlo sampling is costly
- The computational cost is determined by the condition number of the fermion matrix, which scales with the inverse lightest quark mass
- Sign problem at $\mu_B > 0$

Challenges

- Broken symmetries – e.g., Lorentz, chiral
- Fermion doubling
- Grassmann fields (fermions) cannot be sampled, integrate them out:

$$\begin{aligned}\mathcal{Z} &= \int \mathcal{D}[U]\mathcal{D}[\psi]\mathcal{D}[\bar{\psi}]e^{-\mathcal{S}_G[U]-\mathcal{S}_F[\bar{\psi},\psi,U]} \\ &= \int \mathcal{D}[U]e^{-\mathcal{S}_G[U]}\,\mathrm{det}\,|M[U]|\end{aligned}$$

- The effective action is highly non-local, Monte Carlo sampling is costly
- The computational cost is determined by the condition number of the fermion matrix, which scales with the inverse lightest quark mass
- Sign problem at $\mu_B > 0$
- Real-time properties are hard to access

How to access $\mu_B > 0$?

How to access $\mu_B > 0$?

- **Method 1**: Taylor expansion (Allton et al. (2002)), evaluate various derivatives at $\mu = 0$, e.g.

$$\chi_2^u = \frac{T}{V} \left\langle \mathrm{Tr}\left(M_u^{-1} M_u'' - (M_u^{-1} M_u')^2 \right) + \left(\mathrm{Tr}(M_u^{-1} M_u') \right)^2 \right\rangle$$

How to access $\mu_B > 0$?

- **Method 1**: Taylor expansion (Allton et al. (2002)), evaluate various derivatives at $\mu = 0$, e.g.

$$\chi_2^u = \frac{T}{V} \left\langle \mathrm{Tr}\left(M_u^{-1} M_u'' - (M_u^{-1} M_u')^2 \right) + \left(\mathrm{Tr}(M_u^{-1} M_u') \right)^2 \right\rangle$$

- **Method 2**: Perform simulations at imaginary chemical potential, then evaluate the derivatives of $P(i\mu)$ (Lombardo (1999), de Forcrand, Philipsen (2002))

How to access $\mu_B > 0$?

- **Method 1**: Taylor expansion (Allton et al. (2002)), evaluate various derivatives at $\mu = 0$, e.g.

$$\chi_2^u = \frac{T}{V} \left\langle \mathrm{Tr}\left(M_u^{-1} M_u'' - (M_u^{-1} M_u')^2 \right) + \left(\mathrm{Tr}(M_u^{-1} M_u') \right)^2 \right\rangle$$

- **Method 2**: Perform simulations at imaginary chemical potential, then evaluate the derivatives of $P(i\mu)$ (Lombardo (1999), de Forcrand, Philipsen (2002))

- **Methods 3, 4, ...**: Complex Langevin dynamics, contour deformation, reweighting/density of states, ...

Method 1: Taylor expansion

- The chemical potentials for conserved charges B, Q, S:

$$\begin{aligned}
\mu_u &= \frac{1}{3}\mu_B + \frac{2}{3}\mu_Q, \\
\mu_d &= \frac{1}{3}\mu_B - \frac{1}{3}\mu_Q, \\
\mu_s &= \frac{1}{3}\mu_B - \frac{1}{3}\mu_Q - \mu_S
\end{aligned}$$

Method 1: Taylor expansion

- The chemical potentials for conserved charges B, Q, S:

$$\begin{aligned}\mu_u &= \frac{1}{3}\mu_B + \frac{2}{3}\mu_Q,\\ \mu_d &= \frac{1}{3}\mu_B - \frac{1}{3}\mu_Q,\\ \mu_s &= \frac{1}{3}\mu_B - \frac{1}{3}\mu_Q - \mu_S\end{aligned}$$

- The pressure can be expanded in Taylor series

$$\frac{P}{T^4} = \frac{1}{VT^3}\ln \mathcal{Z}(T, V, \hat{\mu}_u, \hat{\mu}_d, \hat{\mu}_s) = \sum_{i,j,k=0}^{\infty} \frac{\chi_{ijk}^{BQS}}{i!j!\,k!}\hat{\mu}_B^i \hat{\mu}_Q^j \hat{\mu}_S^k$$

Method 1: Taylor expansion

- The chemical potentials for conserved charges B, Q, S:

$$\begin{aligned}\mu_u &= \frac{1}{3}\mu_B + \frac{2}{3}\mu_Q,\\ \mu_d &= \frac{1}{3}\mu_B - \frac{1}{3}\mu_Q,\\ \mu_s &= \frac{1}{3}\mu_B - \frac{1}{3}\mu_Q - \mu_S\end{aligned}$$

- The pressure can be expanded in Taylor series

$$\frac{P}{T^4} = \frac{1}{VT^3}\ln \mathcal{Z}(T, V, \hat{\mu}_u, \hat{\mu}_d, \hat{\mu}_s) = \sum_{i,j,k=0}^{\infty} \frac{\chi_{ijk}^{BQS}}{i!j!\,k!}\hat{\mu}_B^i\hat{\mu}_Q^j\hat{\mu}_S^k$$

- The generalized susceptibilities are evaluated at vanishing chemical potential

$$\chi_{ijk}^{BQS} \equiv \chi_{ijk}^{BQS}(T) = \left.\frac{\partial P(T,\hat{\mu})/T^4}{\partial\hat{\mu}_B^i\partial\hat{\mu}_Q^j\partial\hat{\mu}_S^k}\right|_{\hat{\mu}=0}, \quad \hat{\mu} \equiv \frac{\mu}{T}$$

Fluctuations of conserved charges

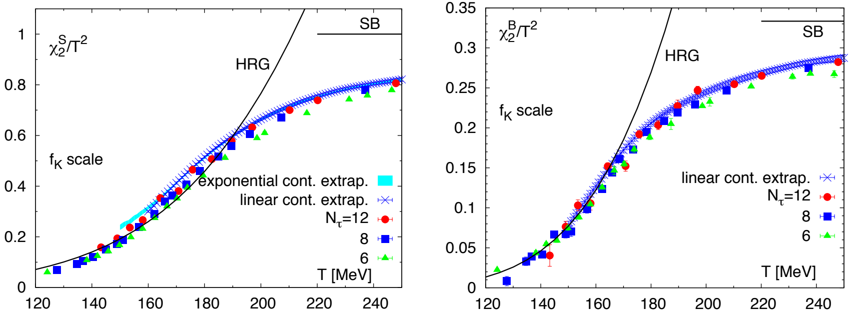

- Strangeness (left) and baryon number (right) fluctuations

Constrained series expansions

- The number densities can also be represented with Taylor expansions:

$$\frac{n_X}{T^3} = \frac{\partial P/T^4}{\partial \hat{\mu}_X}, \ \ X = B, Q, S$$

Constrained series expansions

- The number densities can also be represented with Taylor expansions:

$$\frac{n_X}{T^3} = \frac{\partial P/T^4}{\partial \hat{\mu}_X}, \ \ X = B, Q, S$$

- In heavy-ion collisions there are additional constraints:

$$n_S = 0, \ \ \frac{n_Q}{n_B} = 0.4$$

Constrained series expansions

- The number densities can also be represented with Taylor expansions:

$$\frac{n_X}{T^3} = \frac{\partial P/T^4}{\partial \hat{\mu}_X}, \;\; X = B, Q, S$$

- In heavy-ion collisions there are additional constraints:

$$n_S = 0, \;\; \frac{n_Q}{n_B} = 0.4$$

- These constraints can be fulfilled by

$$\begin{aligned}
\hat{\mu}_Q(T, \mu_B) &= q_1(T)\hat{\mu}_B + q_3(T)\hat{\mu}_B^3 + q_5(T)\hat{\mu}_B^5 + \dots \;, \\
\hat{\mu}_S(T, \mu_B) &= s_1(T)\hat{\mu}_B + s_3(T)\hat{\mu}_B^3 + s_5(T)\hat{\mu}_B^5 + \dots
\end{aligned}$$

Method 2: Imaginary chemical potential[2]

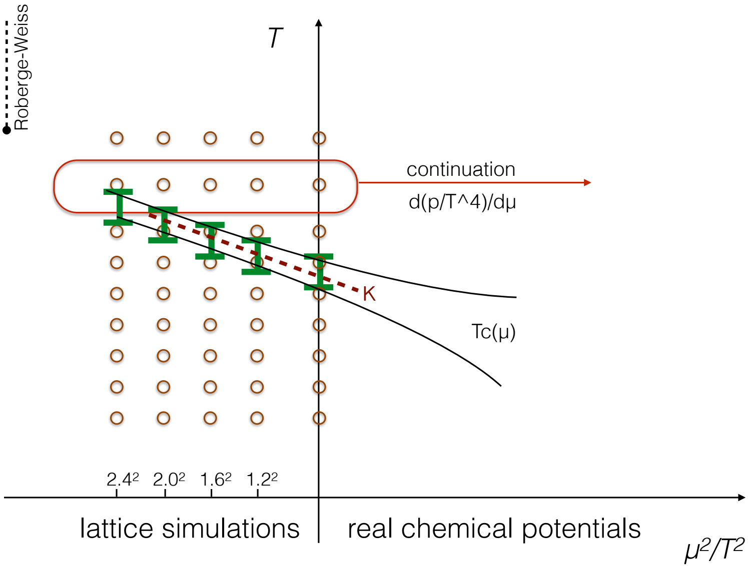

[2]Figure from the talk at Quark Matter 2018 by S. Borsanyi

Baryon number susceptibilities[3]

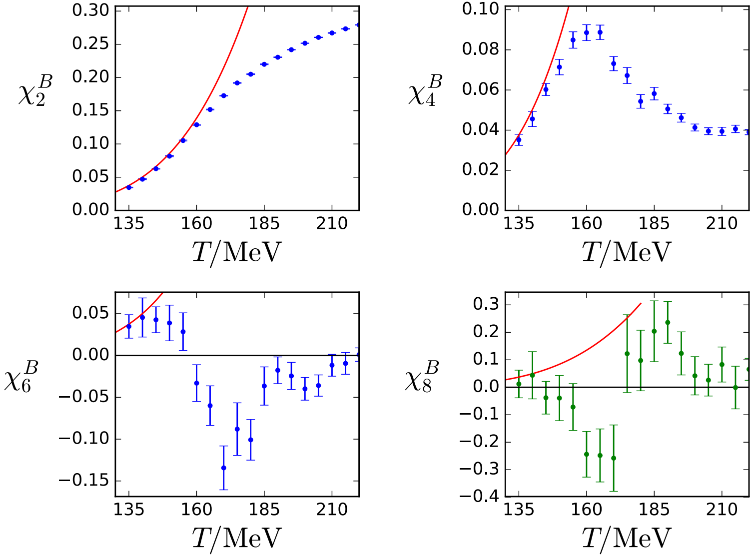

[3] Borsanyi et al. [WB], 1805.04445

Results at $\mu_B = 0$

Chiral symmetry restoration

- Chiral condensate and susceptibility

$$\langle\bar{\psi}\psi\rangle_f = \frac{T}{V}\frac{\partial \ln \mathcal{Z}}{\partial m_f}, \quad \chi(T) = \frac{\partial\langle\bar{\psi}\psi\rangle_f}{\partial m_f}$$

Chiral symmetry restoration

- Chiral condensate and susceptibility

$$\langle\bar{\psi}\psi\rangle_f = \frac{T}{V}\frac{\partial \ln \mathcal{Z}}{\partial m_f}, \quad \chi(T) = \frac{\partial\langle\bar{\psi}\psi\rangle_f}{\partial m_f}$$

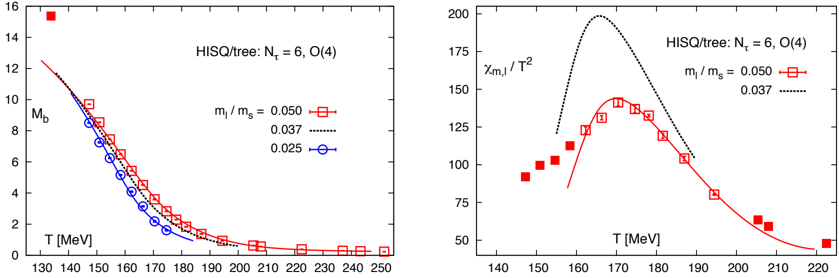

Chiral symmetry restoration

- Chiral condensate and susceptibility

$$\langle\bar{\psi}\psi\rangle_f = \frac{T}{V}\frac{\partial \ln \mathcal{Z}}{\partial m_f}, \quad \chi(T) = \frac{\partial\langle\bar{\psi}\psi\rangle_f}{\partial m_f}$$

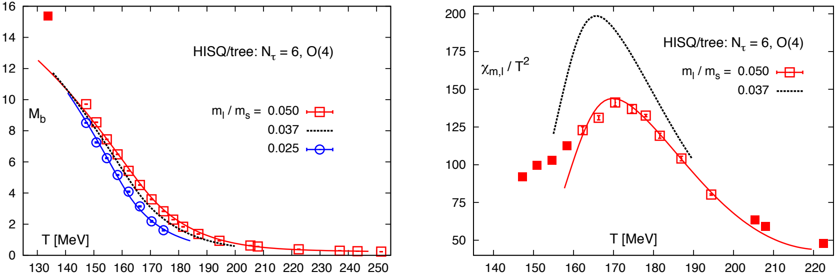

The chiral crossover temperature at $\mu_B = 0$ (Borsanyi et al. [BW] (2010), Bazavov et al. [HotQCD] (2012))

$$T_c = 154 \pm 9 \text{ MeV}$$

Chiral symmetry restoration (update)[4]

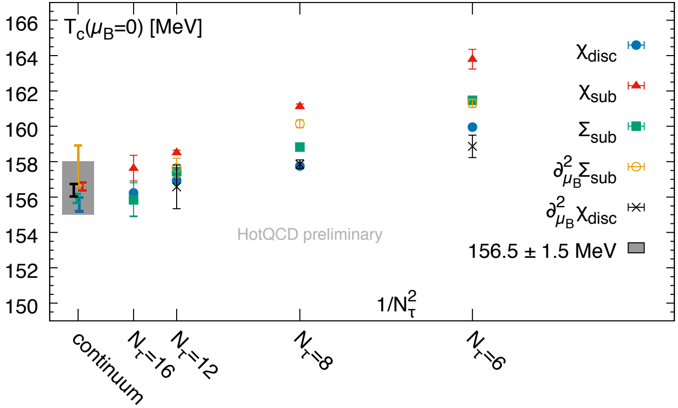

The chiral crossover temperature at $\mu_B = 0$ (HotQCD, preliminary)

$$T_c = 156.5 \pm 1.5 \text{ MeV}$$

[4]Figure from the talk at Quark Matter 2018 by P. Steinbrecher

Chiral symmetry restoration (update)[5]

- Comparison with earlier results

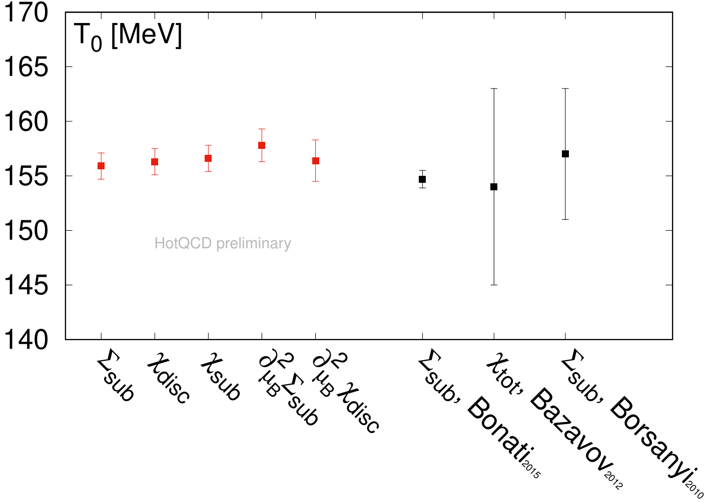

[5]Figure from talk at Quark Matter 2018 by P. Steinbrecher

Results at $\mu_B > 0$

Curvature of the chiral crossover line[6]

- Change in the chiral crossover temperature with μ_B

$$\frac{T_c(\mu_B)}{T_c(0)} = 1 - \kappa_2 \left(\frac{\mu_B}{T_c(0)}\right)^2 - \kappa_4 \left(\frac{\mu_B}{T_c(0)}\right)^4 + O(\mu_B^6)$$

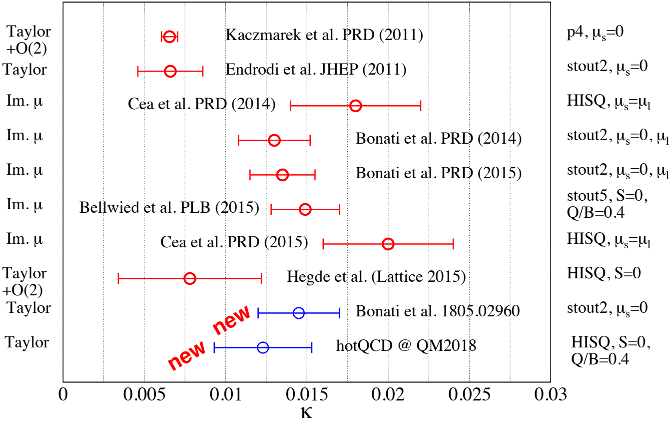

[6]Figure from the talk at Quark Matter 2018 by M. D'Elia

Chiral crossover at $\mu_B > 0$[7]

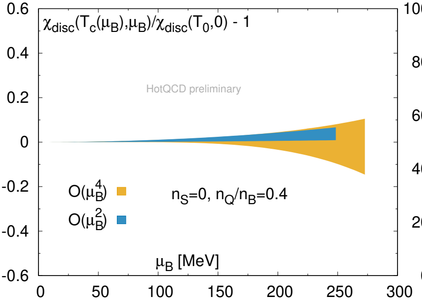

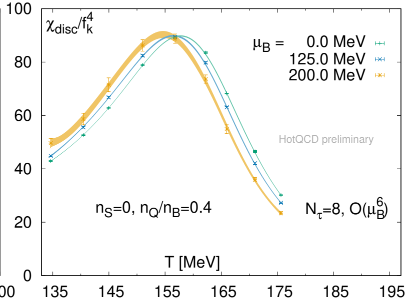

[7] Figure from the talk at Quark Matter 2018 by P. Steinbrecher

Chiral crossover at $\mu_B > 0$[7]

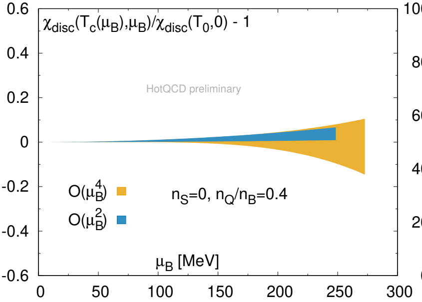

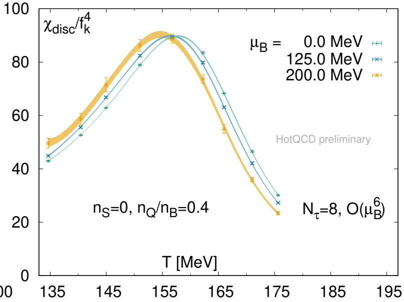

- The magnitude of the chiral susceptibility shows almost no change with increasing $\mu_B > 0$

[7] Figure from the talk at Quark Matter 2018 by P. Steinbrecher

Chiral crossover at $\mu_B > 0$[7]

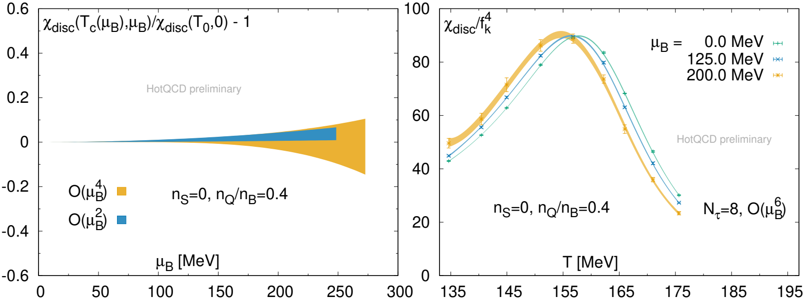

- The magnitude of the chiral susceptibility shows almost no change with increasing $\mu_B > 0$
- No indication that the crossover is getting stronger

[7]Figure from the talk at Quark Matter 2018 by P. Steinbrecher

Chiral crossover at $\mu_B > 0$[7]

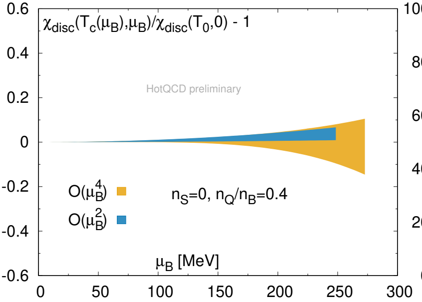

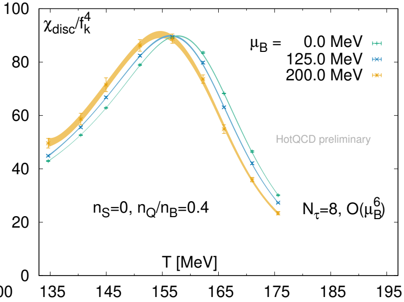

- The magnitude of the chiral susceptibility shows almost no change with increasing $\mu_B > 0$
- No indication that the crossover is getting stronger
- Similar conclusion from the baryon number fluctuations along the crossover line

[7]Figure from the talk at Quark Matter 2018 by P. Steinbrecher

The equation of state at $O(\mu_B^6)$

- The equation of state at $\mu_B = 0$[8]

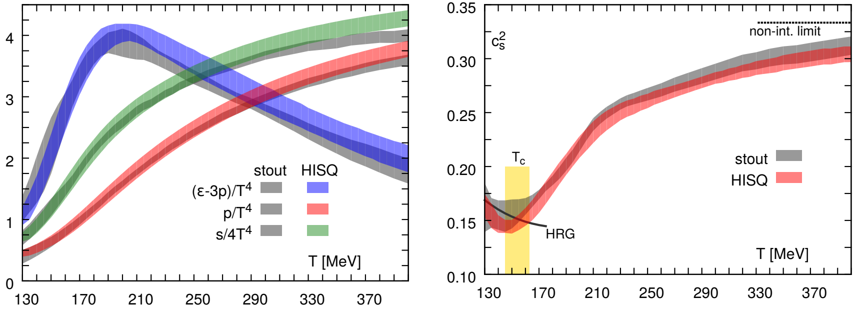

[8] Borsanyi et al. [WB] (2014), Bazavov et al. [HotQCD] (2014)

The equation of state at $O(\mu_B^6)$

- The equation of state at $\mu_B = 0$[8]

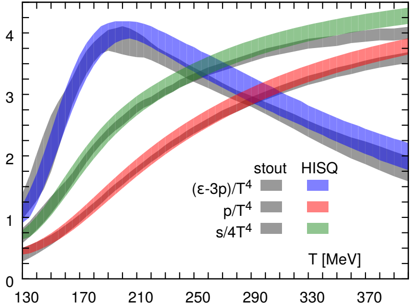

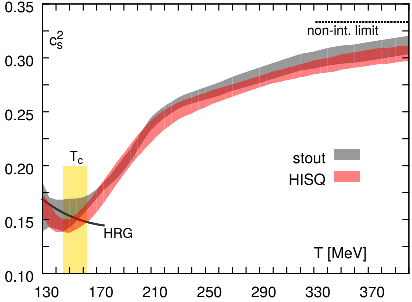

- Additional contribution at $\mu_B > 0$, $\mu_Q = \mu_S = 0$:

$$\frac{\Delta P}{T^4} = \frac{1}{2}\chi_2^B(T)\hat{\mu}_B^2 \left(1 + \frac{1}{12}\frac{\chi_4^B(T)}{\chi_2^B(T)}\hat{\mu}_B^2 + \frac{1}{360}\frac{\chi_6^B(T)}{\chi_2^B(T)}\hat{\mu}_B^4 + \ \ldots\right)$$

[8] Borsanyi et al. [WB] (2014), Bazavov et al. [HotQCD] (2014)

The equation of state at $O(\mu_B^6)$[9]

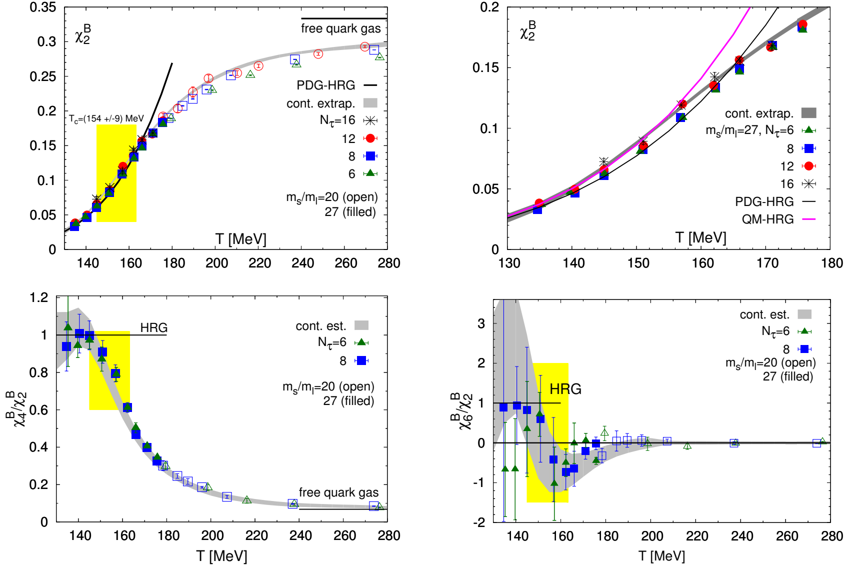

[9] Bazavov et al. [HotQCD] (2017)

The equation of state at $O(\mu_B^6)$

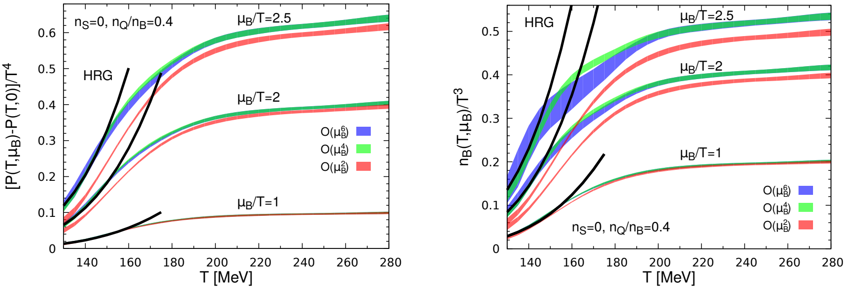

- The contribution to the pressure due to finite chemical potential (left) and the baryon number density (right) for strangeness neutral systems:

$$n_S = 0, \quad \frac{n_Q}{n_B} = 0.4$$

Relativistic heavy-ion collisions

- Cumulants of the event-by-event multiplicity distributions:

$$C_1 = \langle N \rangle \, , \; C_2 = \left\langle (\delta N)^2 \right\rangle , \; C_3 = \left\langle (\delta N)^3 \right\rangle , \; C_4 = \left\langle (\delta N)^4 \right\rangle - 3 \left\langle (\delta N)^2 \right\rangle^2$$

Relativistic heavy-ion collisions

- Cumulants of the event-by-event multiplicity distributions:

$$C_1 = \langle N \rangle \,,\; C_2 = \left\langle (\delta N)^2 \right\rangle ,\; C_3 = \left\langle (\delta N)^3 \right\rangle ,\; C_4 = \left\langle (\delta N)^4 \right\rangle - 3 \left\langle (\delta N)^2 \right\rangle^2$$

- Mean, variance, skewness and kurtosis:

$$M = C_1,\;\; \sigma^2 = C_2,\;\; S = \frac{C_3}{(C_2)^{\frac{3}{2}}},\;\; \kappa = \frac{C_4}{(C_2)^2}$$

Relativistic heavy-ion collisions

- Cumulants of the event-by-event multiplicity distributions:

$$C_1 = \langle N \rangle\,,\ C_2 = \left\langle (\delta N)^2 \right\rangle\,,\ C_3 = \left\langle (\delta N)^3 \right\rangle\,,\ C_4 = \left\langle (\delta N)^4 \right\rangle - 3\left\langle (\delta N)^2 \right\rangle^2$$

- Mean, variance, skewness and kurtosis:

$$M = C_1,\ \ \sigma^2 = C_2,\ \ S = \frac{C_3}{(C_2)^{\frac{3}{2}}},\ \ \kappa = \frac{C_4}{(C_2)^2}$$

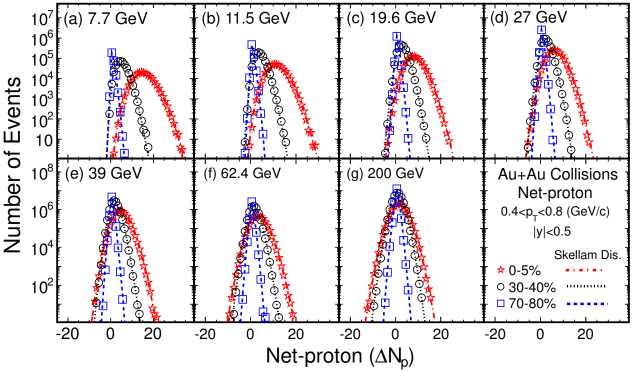

Freeze-out parameters

- Consider the ratios of cumulants:

$$R_{31}^{Q} = \frac{S_Q \sigma_Q^3}{M_Q} = \frac{\chi_3^Q}{\chi_1^Q}, \;\; R_{12}^{Q} = \frac{M_Q}{\sigma_Q^2} = \frac{\chi_1^Q}{\chi_2^Q}$$

[10] Bazavov et al. [BNL-Bielefeld] (2012)

Freeze-out parameters

- Consider the ratios of cumulants:

$$R_{31}^Q = \frac{S_Q \sigma_Q^3}{M_Q} = \frac{\chi_3^Q}{\chi_1^Q}, \quad R_{12}^Q = \frac{M_Q}{\sigma_Q^2} = \frac{\chi_1^Q}{\chi_2^Q}$$

- These ratios can be evaluated on the lattice for constrained system and serve as thermometer (left) and baryometer (right)[10]

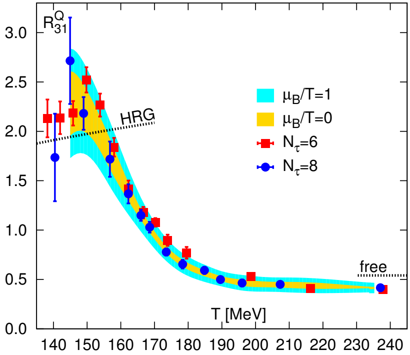

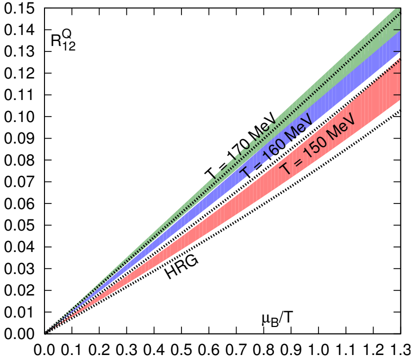

[10] Bazavov et al. [BNL-Bielefeld] (2012)

Skewness and kurtosis

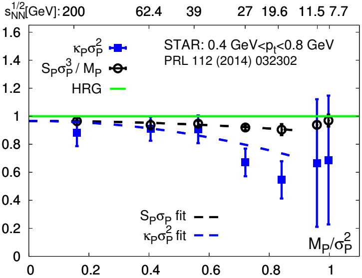

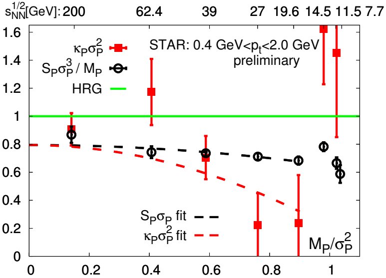

Skewness and kurtosis

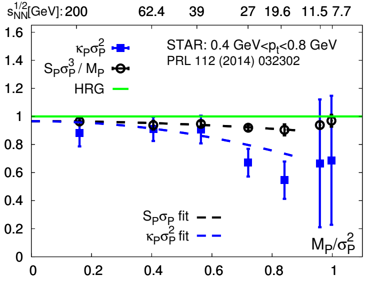

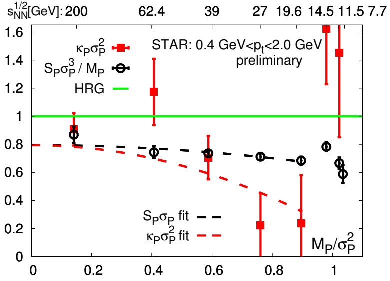

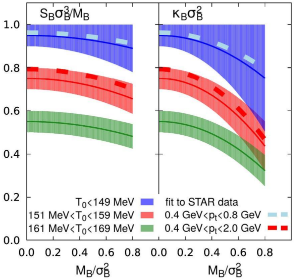

Freeze-out temperatures [BNL-Bielefeld] (2017):

$$T_0 \leq 149 \text{ MeV} \quad \text{for } p_t^{\text{cut}} = 0.8 \text{ GeV}$$

$$T_0 = (153 \pm 5) \text{ MeV} \quad \text{for } p_t^{\text{cut}} = 2.0 \text{ GeV}$$

Skewness and kurtosis

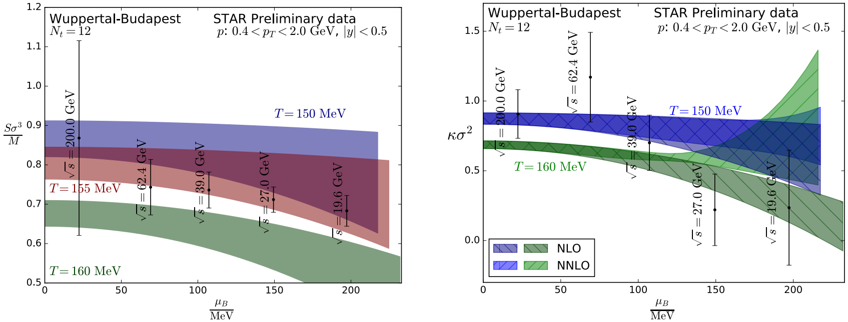

- Recent result by Borsanyi et al. [WB] 1805.04445

Constraints on the critical point

- For $\mu_Q = \mu_S = 0$ the net baryon-number susceptibility is

$$\chi_2^B(T, \mu_B) = \sum_{n=0}^{\infty} \frac{1}{(2n)!} \chi_{2n+2}^B \hat{\mu}_B^{2n}$$

Constraints on the critical point

- For $\mu_Q = \mu_S = 0$ the net baryon-number susceptibility is

$$\chi_2^B(T, \mu_B) = \sum_{n=0}^{\infty} \frac{1}{(2n)!} \chi_{2n+2}^B \hat{\mu}_B^{2n}$$

- The radius of convergence

$$r_{2n}^{\chi} \equiv \sqrt{\frac{2n(2n-1)\chi_{2n}^B}{\chi_{2n+2}^B}}$$

Constraints on the critical point

- For $\mu_Q = \mu_S = 0$ the net baryon-number susceptibility is

$$\chi_2^B(T,\mu_B) = \sum_{n=0}^{\infty} \frac{1}{(2n)!}\chi_{2n+2}^B \hat{\mu}_B^{2n}$$

- The radius of convergence

$$r_{2n}^{\chi} \equiv \sqrt{\frac{2n(2n-1)\chi_{2n}^B}{\chi_{2n+2}^B}}$$

- We observe $\chi_6^B/\chi_4^B < 3$ for $135 < T < 155$ MeV $\Rightarrow r_4^{\chi} \gtrsim 2$

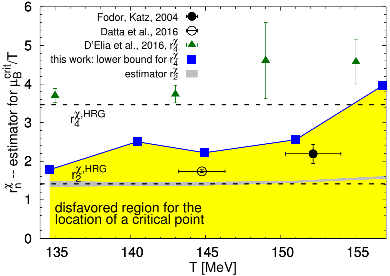

Conclusion

- Lattice QCD calculations are now in the regime of the physical light quark masses and continuum limit is possible for many observables
- The most studied region of the QCD phase diagram is at $\mu_B = 0$
- At non-zero baryon chemical potential direct Monte Carlo simulations are not (yet) possible due to the sign problem
- The region of small μ/T can be explored with expansions in μ/T or by analytic continuation from imaginary μ
- Generalized susceptibilities are now calculated up to 8th order in μ_B
- The equation of state is now known up to the 6th order in μ_B
- Ratios of the generalized susceptibilities can be related to experimentally measured cumulants of event-by-event multiplicity distributions
- Recent lattice calculations strongly disfavor QCD critical point in the region of $\mu_B < 2T$ in the temperature range $135 < T < 155$ MeV